[1.] Abderrazek MESSAOUDI, [1.] László Péter KISS

VIBRATION AND STABILITY OF CURVED BEAMS USING THE FINITE ELEMENT METHOD

[1.] Institute of Applied Mechanics, University of Miskolc, 3515 Miskolc-Egyetemváros, HUNGARY

Abstract: This paper is devoted to the vibration and planar stability of curved beams under a constant concentrated radial load, which is exerted at the crown point. The behavior of the curved beams is analyzed using a one-dimensional model with the help of a commercial finite element software. The results show that the applied method is suitable to predict the behavior of the beams. It turns out that the included angle has a significant influence on the eigenfrequencies and buckling loads. Based on the literature review, this paper aims to tackle vibration and stability problems of a curved beam with I-cross section. The article presents the effect of the included angle on the vibration and stability of fixed-fixed curved beams. The commercial software Abaqus is used to perform the investigations.

Keywords: curved beam; free vibration; eigenfrequency; buckling; FEM

1. INTRODUCTION

Curved beams are elements that can be used in several engineering structures, like in modern bridges, or in lightweight roof structures. As composite engineering components, these can be found, e.g., as wind turbine blades [1]. Since the deformations of a curved beam depend not only on the rotations and radial displacements but also on the tangential displacement caused by the curvature change of the structure, studying the free in-plane vibration of a curved beam using the beam theory is more difficult than studying the equivalent problem in a straight beam [2]. To overcome this complexity and provide engineers with practical knowledge, numerous researchers have examined various aspects of curved beam behavior, and appropriate information on the vibration and stability problems. It is worth noting that one of the most crucial procedures in dynamic structural analysis is free vibration analysis. It determines natural frequencies and vibration modes, which are vital to understand the behavior of any structure subjected to dynamic loads. The finite element method (FEM) is probably the most widely used method, as demonstrated by Petyt and Fleischer [3], who used polynomials and trigonometric form functions to build a thin curved element with two nodes. The finite element method was used to estimate the free vibration of generally curved beams by Yang et al. [2] and Raveendranath et al. [4]. Paper [5] investigated the vibration of simply supported curved beams while taking into account the impact of the curvature on shape modes. For free vibration analysis of arches with non-uniform cross-section, Rossi and Laura [6] also used FEM. In study [7], Auciello and De Rosa compared different estimate approaches for the free vibrations, such as the Ritz method, the Rayleigh–Schmidt method, the Galerkin method, and the finite element method. For both linear and nonlinear elastic buckling, many researchers have reported novel findings. Timoshenko and Gere [8] and Simitses [9] thoroughly investigated the in-plane linear elastic buckling of arches. With respect to the in-plane nonlinear buckling, Pi and Bradford [10,11] addressed the in-plane nonlinear elastic buckling and post-buckling of circular shallow arches, taking into account the pre-buckling deformation effect, and came up with an analytical solutions.

Based on the above literature review, this paper aims to tackle vibration and stability problems of a curved beam with I-cross section. The article presents the effect of the included angle on the vibration and stability of fixed-fixed curved beams. The commercial software Abaqus is used to perform the investigations.

2. NUMERICAL EVALUATIONS

Figure 1a shows the considered beam with an arch length S of 21740 mm. The beam has ideal fixed supports at the ends. It is assumed that the material is isotropic and homogeneous, which means that the modulus of elasticity E and the Poisson ratio ν are constant over the whole arch: $E=E_{STEEL}=2.1e5$ N/mm^2, $\nu=0.3$. The material density is 7830 kg/m^3 The axial coordinate z coincides with the centroid of each cross-section, while the transverse coordinates are x and y. F is a constant, vertical concentrated radial load at the crown point.

The detailed geometrical data of the doubly symmetric I- cross section are shown in Figure 1b. The section depth (h) is 256 mm, flange width ($b_1=b_2$) is 146 mm, flange thickness ($t_1=t_2$) is 10.9 mm, and the web thickness is $t_3=6$ mm.

ISSN 1584 – 2665 (printed version); ISSN 2601 – 2332 (online); ISSN-L 1584 – 2665

A one-dimensional model is applied in the selected FE software to analyze the dedicated problem. In all calculations, 100 elements of type B21 are used to obtain converged results of the physical problem.

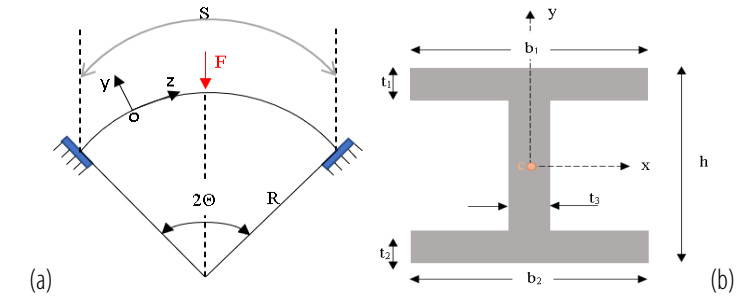

Figure 1. (a) Fixed-fixed curved beam under a constant concentrated vertical load at the crown point, (b) the I-shaped cross-section

FREE VIBRATIONS

We assumed no external force was applied to the curved beam (F=0) for free vibrations. The results of the three lowest natural frequencies as functions of the included angle 2Θ are presented in Table 1 as long as 2Θ=[0.5;4.0] rad. It can be seen that the first natural frequency continuously decreases as the included angle increases. When 2Θ<=1.5 rad, the second and third eigenfrequencies increase as the included angle increases, however, they decrease significantly when 2Θ>=1.5 rad.

Table 1. Solutions for the eigenfrequencies in [Hz]

Eigenfrequency \ 2Θ [rad]	0.5	1	1.5	2	3	4
1st eigenfrequency	11.455	11.084	10.541	9.878	8.334	6.794
2nd eigenfrequency	15.057	19.405	19.586	19.227	17.900	16.161
3rd eigenfrequency	24.265	35.387	35.698	34.915	32.916	30.595

When 2Θ =1.5 rad, the three mode shapes are displayed in Figure 2. The second mode is a symmetric function.

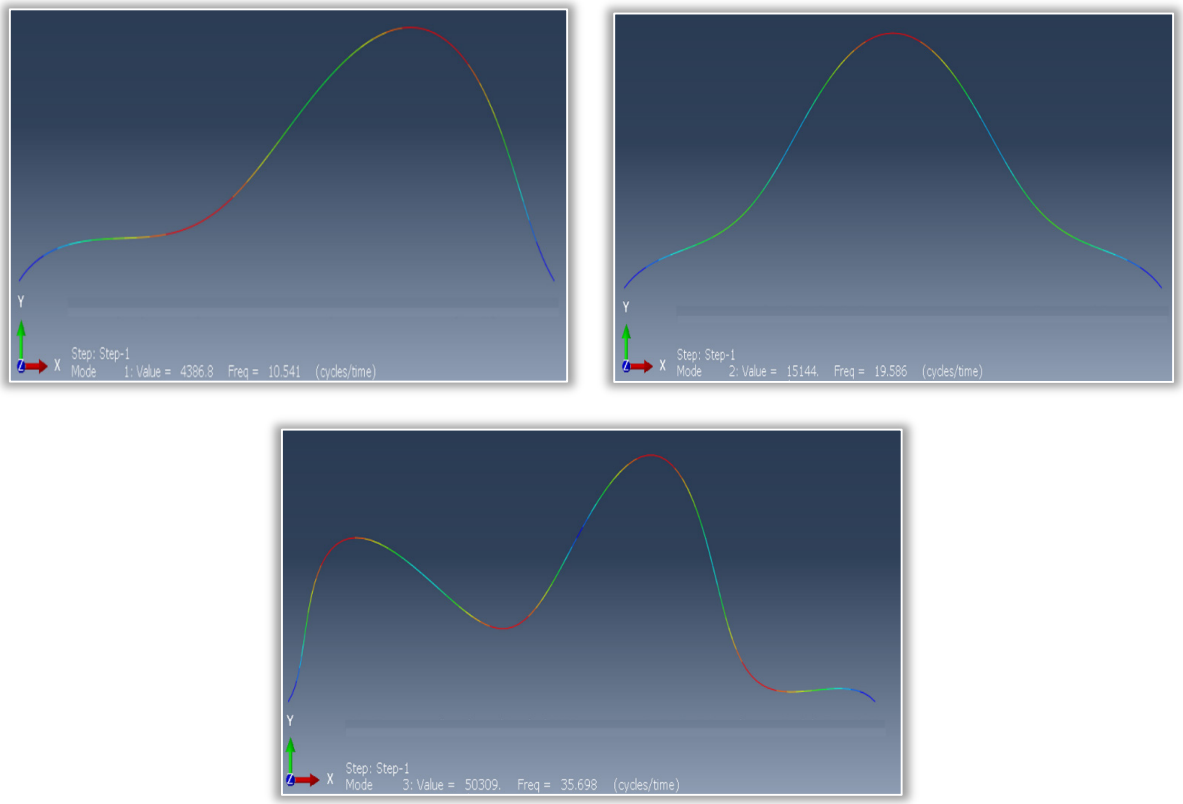

Figure 2. The first three mode shapes when 2θ =1.5 rad

STABILITY PROBLEM

The aim of the section is to investigate the influence of the applied force on the displacements of the beam, in order to determine the critical values where limit point buckling happens. For certain deep arches, linear buckling models might be sufficient to predict the ultimate load. However, the nonlinear material model is preferred to be used for a better accuracy. A chart presenting the relationship between loads and displacements is undertaken to perform a geometrically nonlinear solution using an arc-length method (Riks algorithm). We shall give an example of how to determine the non-linear buckling values using this

ISSN 1584 – 2665 (printed version); ISSN 2601 – 2332 (online); ISSN-L 1584 – 2665

algorithm. When 2Θ=1.5, the load values against the displacement for 38 increments are presented in Table 2. The maximum force has a value of 1.059e6 N and the corresponding vertical crown point displacement is 1.48e3 mm.

Table 2. Displacement-load values when 2Θ=1.5 rad

Displ.*10³(mm)	Load*10⁶(N)	Displ.*10³(mm)	Load*10⁶(N)
0.00E+00	0	0.96	1.01
3.50E-07	1E-06	1.02	1.02
3.19E-06	9.1E-06	1.05	1.03
1.16E-05	3.3E-05	1.09	1.04
6.02E-05	0.00	1.24	1.05
1.36E-04	0.00	1.48	1.059
2.04E-04	0.00	1.48	1.058
1.03E-03	0.00	1.48	1.058
2.33E-03	0.01	1.58	1.05
0.01	0.01	1.72	1.04
0.03	0.09	1.81	1.03
0.04	0.10	1.91	1.02
0.37	0.67	1.96	1.01
0.38	0.67	2.07	0.99
0.51	0.79	2.12	0.98
0.51	0.80	2.15	0.98
0.87	0.98	2.18	0.97
0.87	0.98	2.23	0.96
0.96	1.01	2.25	0.96

In accordance with the output data in Table 2, Figure 3 shows the displacement values (on the horizontal axis) against the force (on the vertical axis). The upper limit point of the nonlinear equilibrium path is obtained when the force reaches its maximum on the primary stable branch. According to the Riks algorithm, this maximum force is the nonlinear buckling load sought. This principle is used to perform the nonlinear analysis for each angle.

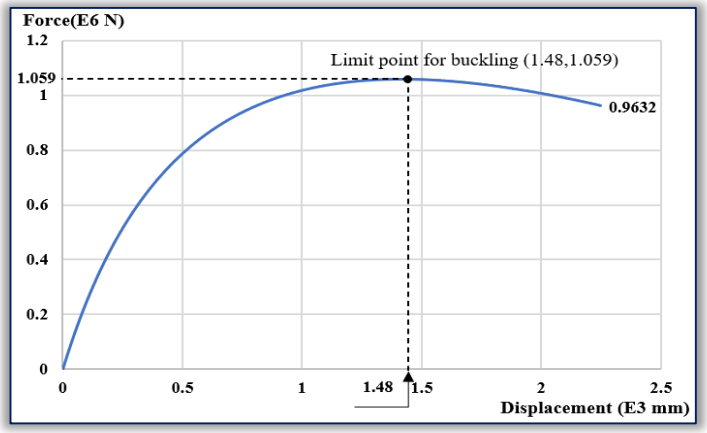

Figure 3. Relationship between loads and displacements when 2Θ=1.5 rad

Moving on now to the geometrically linear and nonlinear stability analyses, Table 3 shows the variation of the buckling loads as function of the included angle. N_{lin} denotes the lowest linear buckling load, while N_{nlin} denotes the nonlinear buckling load. We shall introduce a dimensionless critical load $Q= N_{lin}/ N_{nlin}$ to study the effect nonlinearities and the included angle on the stability problem.

Table 3. Linear and non-linear critical loads

Included angle 2θ [rad]	0.5	1	1.5	2	3	4
Linear buckling load, N_{lin} *10⁶[N]	0.519	1.062	1.611	2.189	3.328	3.872
Non-Linear buckling load, N_{nlin} *10⁶[N]	0.309	0.682	1.058	1.432	2.278	3.361
Q [-]	1.682	1.558	1.522	1.528	1.461	1.152

It can be observed that as the angle 2Θ is increased, the critical load in the case of nonlinear analysis is 40.5-13.2 % lower than the outcome from linear buckling analysis. So it can be concluded that the linear model dangerously overestimates the maximum allowable load. The error is greater for lower angles, i.e., for shallow arches. As demonstrated in Figure 4, the dimensionless critical load ratio Q decreases significantly while the included angle is increased. The plotted relationship is non-linear. The discrete points of Q are denoted by diamonds, and the continuous line is drawn by using a polynomial that fits onto the discrete points with two-to-three-digit accuracy.

ISSN 1584 – 2665 (printed version); ISSN 2601 – 2332 (online); ISSN-L 1584 – 2665

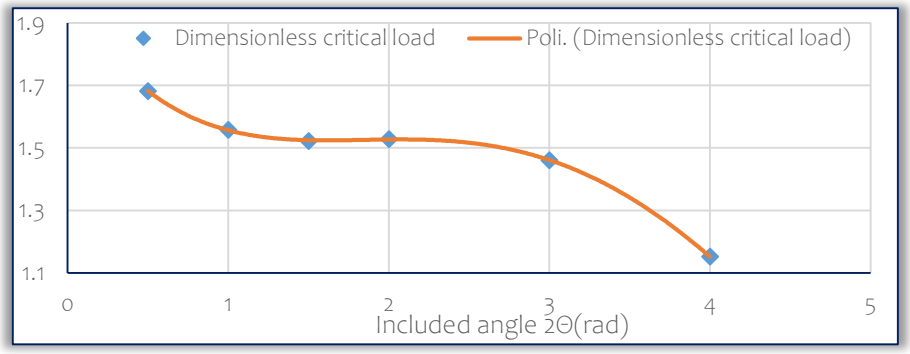

Figure 4. Dimensionless critical loads against 2θ

The following polynomial is fitted onto the discrete point values presented in Table 3.

$$Q = 0.0106(2\Theta)^4 - 0.1403(2\Theta)^3 + 0.5554(2\Theta)^2 - 0.8674(2\Theta) + 1.9955\,. \qquad (1)$$

VIBRATIONS OF PRE-LOADED CURVED BEAMS

In order to investigate the behavior of a loaded curved beams under a constant concentrated load, the applied force was set equal to 0,10,…,90% of the nonlinear buckling load (N_{nlin}) in order to avoid the buckling phenomenon. We shall take an example where 2Θ=1.5 and based on Table 2, the nonlinear critical load is equal to 1.059e6 N. The effect of this load portion (in shorter, Lp) on the three first three eigenfrequencies is presented in Table 4. Here, k= 1,2,3 is the mode number.

It can be observed that the second column in Table 4 represents the eigenfrequencies for the unloaded beams (the same results as in Table 1) and these values decrease gradually with the increase of the load level. Figure 5 shows the variation of the first natural frequencies W_1 of the loaded curved beams against the included angle variation for five L_P load portion values.

Table 4. The effect of the applied force on the eigenfrequencies when 2θ=1.5

Lp of 1.059 e6 N	0	0.1	0.2	0.3	0.4	0.5	0.6	0.7	0.8	0.9
1st freq. [Hz]	10.557	10.193	9.812	9.412	8.992	8.538	8.049	7.513	6.887	6.104
2nd freq. [Hz]	19.613	18.752	17.818	16.802	17.700	14.741	13.119	11.611	9.813	7.536
3rd freq. [Hz]	35.748	35.227	34.682	34.109	33.504	32.847	32.135	31.346	30.409	29.21

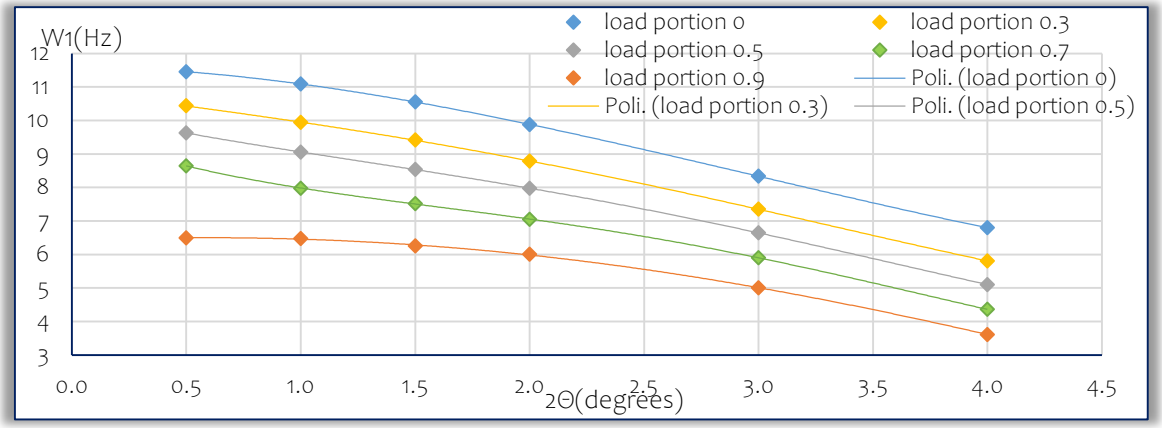

Figure 5. First natural frequency against included angle for different values of Lp

Polynomial (2) is fitted onto the discrete values of W_1(Lp=0,0.3,0.5,0.7,0.9):

$$W_1(Lp=0,2\Theta)=0.0003(2\Theta)^4+0.056(2\Theta)^3-0.515(2\Theta)^2-0.057(2\Theta)+11.6,\ 2\Theta \in [0.5,4.0] \qquad (2a)$$

$$W_1(Lp=0.3,2\Theta)=0.0105(2\Theta)^4-0.074(2\Theta)^3+0.04(2\Theta)^2-0.918(2\Theta)+10.89,\ 2\,\Theta \in [0.5,4.0] \qquad (2b)$$

$$W_1(Lp=0.5,2\Theta)=0.02(2\Theta)^4-0.193(2\Theta)^3+0.534(2\,\Theta)^2-1.634(2\,\Theta)+10.33,\ 2\Theta \in [0.5,4.0] \qquad (2c)$$

$$W_1(Lp=0.7,2\Theta)=0.0363(2\,\Theta)^4-0.387(2\Theta)^3+1.3(2\Theta)^2-2.665(2\Theta)+9.7,\ 2\Theta \in [0.5,4.0] \qquad (2d)$$

$$W_1(Lp=0.9,2\Theta)=0.003(2\Theta)^4-0.017(2\Theta)^3-0.23(2\Theta)^2+0.28(2\Theta)+6.418,\ 2\Theta \in [0.5,4.0] \qquad (2e)$$

A force equal to 50% of the non-linear buckling load is applied to the curved beam when the angle is 1.5 rad to reveal the differences in terms of natural frequencies between the loaded and unloaded beams. These differences are compared in Table 5. With a value of 26.27%, the second mode relates to the largest difference, followed by 18.46 % and 8.13 % in the first and third modes, respectively.

Figure 6 depicts the first three mode shapes of the loaded beam with Lp=0.5 and 2Θ=1.5 rad. These are directly comparable with the unloaded shapes of Figure 2.

ISSN 1584 – 2665 (printed version); ISSN 2601 – 2332 (online); ISSN-L 1584 – 2665

Table 5. Difference of eigenfrequencies in % between unloaded & loaded beams

2Θ=1.5 rad	W_1 [Hz]	W_2 [Hz]	W_3 [Hz]
Unloaded beam(F=0)	10.451	19.586	35.698
Pre-loaded beam (F=0.5295e6 N)	8.521	14.441	32.795
Difference (%)	18.46	26.27	8.13

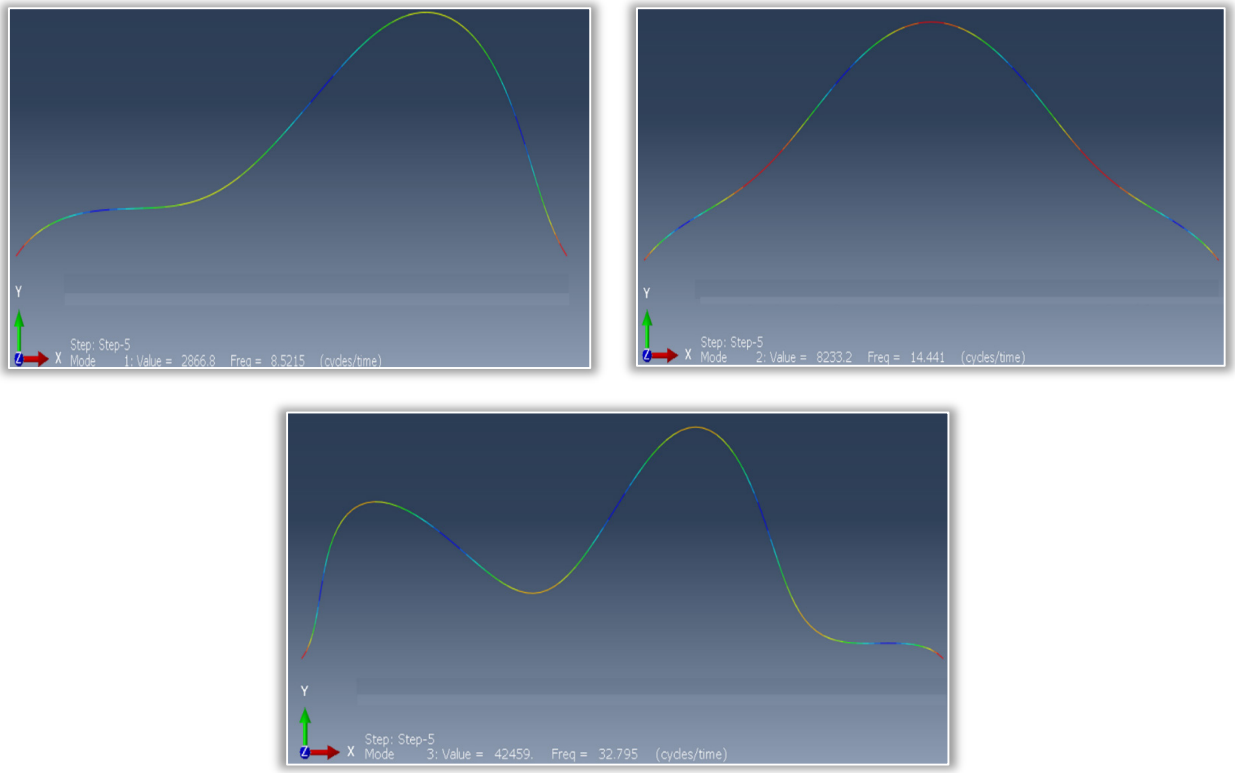

Figure 6. First three mode shapes for a loaded curved beam with Lp=0.5

The effect of Lp on the first three eigenfrequency ratios $W_k/\hat{W}_k$ is shown in Figures 7,8 and 9 where k is the mode number (k=1,2,3). W_k and $\hat{W}_k$ represent the eigenfrequency value of the loaded and unloaded beams, respectively.

Polynomials (3), (4), and (5) are fitted onto the discrete values of $W_k/\hat{W}_k$ (k=1,2,3). Parameter x represents the portion of buckling load. The calculations are performed for three different included angles. The principle of the calculations is the same for any $2\Theta \in [0.5,4.0]$. Polynomials for the first dimensionless eigenfrequency ratio $W_1/\hat{W}_1$:

$$W_1/\hat{W}_1(2\Theta=0.5,x)=-13.78x^6+31.78x^5-27.45x^4+10.81x^3-1.99x^2-0.16x+0.9998,\ x\in[0,0.9] \quad (3a)$$

$$W_1/\hat{W}_1(2\Theta=1,x)=-1.702x^6+4.05x^5-3.807x^4+1.655x^3-0.436x^2-0.286x+1 \quad x\in[0,0.9] \quad (3b)$$

$$W_1/\hat{W}_1(2\Theta=4,x)=1.329x^6-3.13x^5+2.737x^4-1.09x^3+0.13x^2-0.478x+1 \quad x\in[0,0.9] \quad (3c)$$

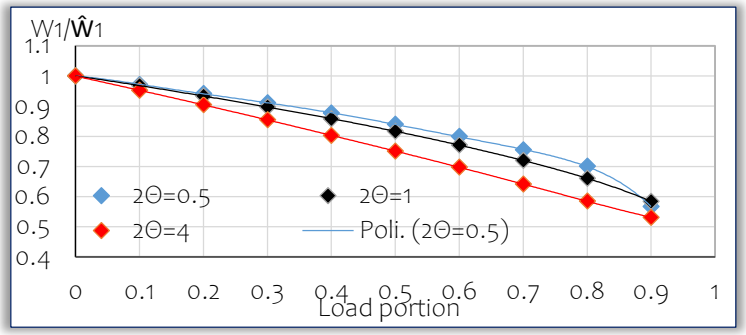

Figure 7. Function $W_1/\hat{W}_1$ against load portion

Polynomial for the second dimensionless eigenfrequency ratio $W_2/\hat{W}_2$:

$$W_2/\hat{W}_2(2\Theta=0.5,x)=9.916x^6-23.8x^5+21.08x^4-8.61x^3+1.37x^2-0.446x+1;\ x\in[0,0.9] \quad (4a)$$

$$W_2/\hat{W}_2(2\Theta=1,x)=-2.906x^6+6.98x^5-6.5504x^4+2.8495x^3-0.7667x^2-0.3864x+1;\ x\in[0,0.9] \quad (4b)$$

$$W_2/\hat{W}_2(2\Theta=4,x)=-2.74x^6+11.75x^5-20.14x^4+16.39x^3-6.42x^2+0.476x+0.9996;\ x\in[0,0.9] \quad (4c)$$

ISSN 1584 – 2665 (printed version); ISSN 2601 – 2332 (online); ISSN-L 1584 – 2665

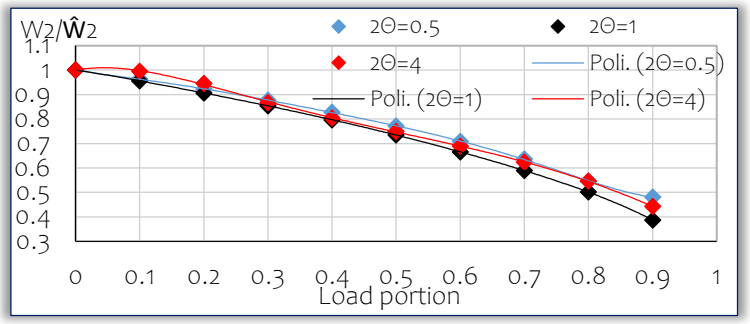

Figure 8. Function $W_2/\hat{W}_2$ against load portion

Polynomial for the third dimensionless eigenfrequency ratio $W_3/\hat{W}_3$:

$$W_3/\hat{W}_3(2\Theta=4,x)=0.804x^6-1.51x^5+1.173x^4-0.3604x^3+0.164x^2+0.0197x+1;\ x\in[0,0.9] \quad (5a)$$

$$W_3/\hat{W}_3(2\Theta=4,x)=-6.496x^6+19.48x^5-22.99x^4+13.411x^3-4.034x^2+0.437x+1;\ x\in[0,0.9] \quad (5b)$$

$$W_3/\hat{W}_3(2\Theta=4,x)=-6.27x^6+20.73x^5-26.87x^4+16.954x^3-5.22x^2+0.364x+0.9998;\ x\in[0,0.9] \quad (5c)$$

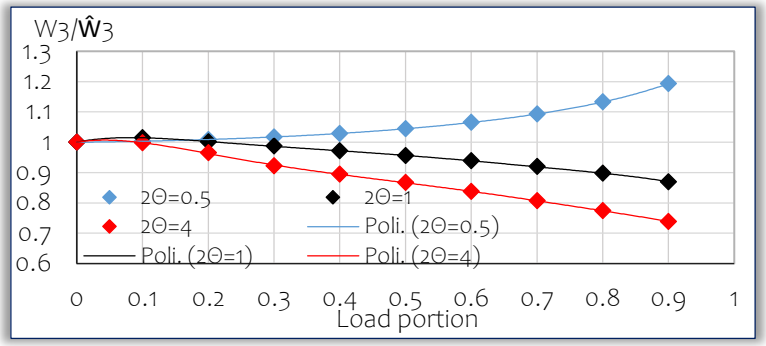

Figure 9. Function $W_3/\hat{W}_3$ against load portion

3. CONCLUSIONS

In this paper, a finite element analysis was applied to study the in-plane vibration and stability of fixed-fixed beams with I cross-section. The eigenfrequency solutions of the unloaded/pre-loaded beams were also obtained. Since the model is developed for fixed-fixed curved beams, the dependence of eigenfrequencies/buckling loads on the included the angle of the beam has been investigated. It turned out that (1) when 2Θ=[0.5,4.0], the first natural frequency decreased as the included angle is increased. (2) When 2Θ<=1.5 rad, the second and third eigenfrequencies increased as the included angle increased, however, they decreased significantly when 2Θ>=1.5rad. (3) The dimensionless critical buckling load ratio Q decreased significantly as the included angle increased.

References

[1] Abbey,T.: Linear and Nonlinear Buckling in FEA, 2015., https://www.digitalengineering247.com/article/linear-and-nonlinear-buckling-in-fea/
[2] Yang, F., Sedaghati, R., Esmailzadeh, E.: Free in-plane vibration of general curved beams using finite element method. Journal of Sound and Vibration, 318, 850–867, 2008.
[3] Petyt, M., Fleischer, C.C.: Free vibration of a curved beam, Journal of Sound and Vibration, 18(1), 1–30, 1971.
[4] Raveendranath, P., Singh, G., Pradhan, B.: Free vibration of arches using a curved beam element based on a coupled polynomial displacement, Computers & Structures, 78, 583–590, 2000.
[5] Nicoletti, R.: On the natural frequencies of simply supported beams curved in mode shapes, Journal of Sound Vibration, 485, 115597, 2020.
[6] Rossi, R. E., Laura, P.A.A.: Dynamic stiffening of an arch clamped at one end and free at the other, Journal of Sound and Vibration, 160, 190–192, 1993.
[7] Auciello, N. M., De Rosa, M. A.: Free vibrations of circular arches: a review. Journal of Sound and Vibration, 4(176), 433–458, 1994.
[8] Timoshenko, S. P., Gere, J.M.: Theory of Elastic Stability, McGraw-Hill International Book Company, 1963.
[9] Simitses, G. J.: An introduction to the elastic stability of structures, Journal of Applied Mechanics, 43(2), 383-384, 1976.
[10] Bradford, M. A., Uy, B., Pi ,Y.-L.: In-plane elastic stability of arches under a central concentrated load, Journal of Engineering Mechanics, ASCE, 128(7), 710, 2002.
[11] Pi, Y.-L., Bradford, M. A., Uy, B.: In-plane stability of arches, International Journal of Solids and Structures, 39, 105–125, 2002.

ISSN 1584 – 2665 (printed version); ISSN 2601 – 2332 (online); ISSN–L 1584 – 2665